

RECEIVED: January 14, 2025 ACCEPTED: April 9, 2025 PUBLISHED: May 9, 2025

Search for K_S^0 invisible decays



The BESIII collaboration

E-mail: besiii-publications@ihep.ac.cn

ABSTRACT: Based on $(1.0087 \pm 0.0044) \times 10^{10}~J/\psi$ events collected with the BESIII detector at the BEPCII e^+e^- storage ring, we search for K^0_S invisible decays via the $J/\psi \to \phi K^0_S K^0_S$ process. No significant signal is observed, and the upper limit of the branching fraction of these invisible decays is set at 8.4×10^{-4} at the 90% confidence level. This is the first experimental search for K^0_S invisible decays.

Keywords: Beyond Standard Model, Branching fraction, Dark Matter, e^+-e^- Experiments

ARXIV EPRINT: 2501.06426

Contents

1	Introduction	1	
2	BESIII detector and Monte Carlo simulation	2	
3	Analysis method	3	
4	Event selection and data analysis	4	
5	Background analysis	6	
6	Systematic uncertainties	8	
7	Result	8	
8	Summary	10	
\mathbf{T}	The BESIII collaboration		

1 Introduction

The Standard Model (SM) of particle physics has been a cornerstone in understanding the subatomic world over the past several decades, providing a comprehensive framework for explaining many observed phenomena. Despite its extensive successes, the SM does not address certain issues, most notably dark matter [1]. Accumulating indirect evidence from astronomical and cosmological observations strongly suggests the existence of dark matter [2, 3], which is invisible in the entire electromagnetic spectrum, and its existence is inferred via gravitational effects only so far. Studies of invisible decays, where particles decay into final states that do not produce detectable signals, are therefore important for the development of SM extensions [4, 5].

Stringent limits on the invisible decays of the Υ [6], J/ψ [7], B^0 [8], B_s [9], $\eta(\eta')$ [10–12], π^0 [13], D^0 [14], ω [15], ϕ [15] mesons and the Λ [16] baryon have already been set by several experiments. However, no experimental study of fully-invisible decays of kaons has been performed yet. Within the SM, the branching fraction (BF) of $K_S^0 \to \nu \bar{\nu}$ decay is predicted to be extremely small. This process is kinematically forbidden under the assumption of massless neutrinos due to angular momentum conservation, and remains highly suppressed in the case of massive neutrinos due to the unfavorable helicity configuration, with a BF smaller than 10^{-16} [18]. Consequently, the search of the K_S^0 invisible decay offers a sensitive test of the SM [5].

By summing all the known K_S^0 decay modes reported in PDG [17], an indirect estimation of the BF allowing K_S^0 to decay invisibly is established at the order of 10^{-4} [18]. Additionally, theories like the mirror-matter model [19, 20], which assumes the existence of a mirror world parallel to our own, suggest that the K_S^0 invisible decay could be interpreted as an oscillation between normal and mirror particles, and predict the BF of $K_S^0 \to \text{invisible}$ to be at the order of 10^{-6} . As there has been no experimental exploration of $K_S^0 \to \text{invisible}$ reported, the indirect experimental upper limit (UL) and the model prediction both remain unverified.

It's worth noting that $K_S^0 \to \text{invisible}$, also a flavor-changing neutral current kaon decay with missing energy, can provide complementary probes of new physics in the $s \to d$ transitions [21]. Besides, study of the K_S^0 invisible decay is also essential for testing CPT invariance [18]. Using the neutral kaon system for such tests offers advantages over the B^0 or D^0 meson systems; specifically, one benefits from the small total decay widths and the limited number of significant (hadronic) decay modes [22]. The Bell-Steinberger relation (BSR) [23], derived from the requirement of unitarity, connects potential CPT-invariance violation to the amplitudes of all decay channels of neutral kaons. Although the BSR provides the most sensitive test of CPT symmetry, previous BSR tests with neutral kaons have been conducted assuming that there is no contribution from invisible decay modes.

In this paper, we report the first experimental search for K_S^0 invisible decays via the $J/\psi \to \phi K_S^0 K_S^0$ decay, by analyzing $(1.0087 \pm 0.0044) \times 10^{10} \ J/\psi$ events collected with the BESIII detector at the BEPCII e^+e^- storage ring [24]. The usage of $J/\psi \to \phi K_S^0 K_S^0$, where one of the K_S^0 is reconstructed through its decay to $\pi^+\pi^-$, provides a unique advantage for probing K_S^0 invisible decays. Most J/ψ decay modes with K_S^0 in the final states suffer from high contamination from K_L^0 background, which can mimic the signal as they rarely interact. In contrast, in $J/\psi \to \phi K_S^0 K_S^0$ decay, with a BF of $(5.9 \pm 1.5) \times 10^{-4}$ [17], one of the dominant K_L^0 backgrounds, $J/\psi \to \phi K_S^0 K_L^0$ is forbidden by C-parity conservation. This enables us to probe the K_S^0 invisible decay signal from a relatively clean K_S^0 sample.

2 BESIII detector and Monte Carlo simulation

The BESIII detector [25] records symmetric e^+e^- collisions provided by the BEPCII storage ring [26] in the center-of-mass energy range from 1.84 to 4.95 GeV, with a peak luminosity of 1.1×10^{33} cm⁻²s⁻¹ achieved at $\sqrt{s} = 3.773$ GeV. BESIII has collected large data samples in this energy region [27]. The cylindrical core of the BESIII detector covers 93% of the full solid angle and consists of a helium-based multilayer drift chamber (MDC), a plastic scintillator time-of-flight system (TOF), and a CsI(Tl) electromagnetic calorimeter (EMC), which are all enclosed in a superconducting solenoidal magnet providing a 1.0 T magnetic field. The magnetic field was 0.9 T in 2012, which affects 11% of the total J/ψ data. The solenoid is supported by an octagonal flux-return yoke with resistive plate counter muon identification modules (MUC) interleaved with steel.

The charged-particle momentum resolution at 1 GeV/c is 0.5%, and the specific ionization energy loss ($\mathrm{d}E/\mathrm{d}x$) resolution is 6% for electrons from Bhabha scattering. The EMC measures photon energies with a resolution of 2.5% (5%) at 1 GeV in the barrel (end-cap) region. The time resolution in the TOF barrel region is 68 ps, while that in the end-cap region is 110 ps. The end-cap TOF system was upgraded in 2015 using multi-gap resistive plate chamber

technology, providing a time resolution of 60 ps, which benefits 87% of the data used in this analysis [28, 29].

Simulated data samples produced with the GEANT4-based [30] Monte Carlo (MC) package, which includes the geometric and material description of the BESIII detector [31–33] and the detector response, are used to determine detection efficiencies and to estimate backgrounds. The simulation models the beam energy spread and initial state radiation in the e^+e^- annihilations with the generator KKMC [34, 35]. The inclusive MC sample includes the production of the J/ψ resonance incorporated in KKMC. All particle decays are modeled with EVTGEN [36, 37] using the BFs either taken from the Particle Data Group (PDG) [17], when available, or otherwise estimated with LUNDCHARM [38, 39]. Final state radiation from charged final state particles is incorporated using the PHOTOS package [40]. The signal MC sample for $J/\psi \to \phi K_S^0 K_S^0$ is generated using a phase space model. To better model the intermediate resonance contributions to the $J/\psi \to \phi K_S^0 K_S^0$ final state, a multidimensional re-weighting method as described in ref. [41] is employed. Detailed information about this re-weighting method is provided in section 4.

3 Analysis method

In this analysis, the K_S^0 sample is selected using the $J/\psi \to \phi K_S^0 K_S^0$ process. To study the $K_S^0 \to \text{invisible}$ without relying on the BF of $J/\psi \to \phi K_S^0 K_S^0$, which suffers from significant uncertainties, a novel method is employed. In this method, we define a normalization sample first, containing the events that satisfy $J/\psi \to \phi K_S^0 K_S^0$, $\phi \to K^+ K^-$, $K_S^0 \to \pi^+ \pi^-$ with the K_S^0 in the recoiling system decaying to processes other than $\pi^+\pi^-$. The K_S^0 decaying to $\pi^+\pi^-$ is denoted as K_S^0 (tag) hereafter. Each event in this sample inherently qualifies as a candidate for the K_S^0 invisible decay, since it only contains four charged particles. Subsequently, we can probe the $K_S^0 \to \text{invisible}$ decay using the identical dataset, where the $K_S^0 \to \text{invisible}$ candidate is searched for in the system recoiling against a reconstructed ϕK_S^0 candidate.

The yields for the selected normalization sample and the $K_S^0 \to \text{invisible signal events}$ are denoted as $N_{\text{norm.}}$ and N_{signal} , which are given by:

$$N_{\text{norm.}} = 2 \times N_{J/\psi \to \phi K_S^0 K_S^0} \times \mathcal{B}(\phi \to K^+ K^-) \times \mathcal{B}(K_S^0 \to \pi^+ \pi^-) \times (1 - \mathcal{B}(K_S^0 \to \pi^+ \pi^-)) \times \varepsilon_{\text{norm.}},$$
(3.1)

and

$$N_{\text{signal}} = 2 \times N_{J/\psi \to \phi K_S^0 K_S^0} \times \mathcal{B}(\phi \to K^+ K^-) \times \mathcal{B}(K_S^0 \to \pi^+ \pi^-)$$
$$\times \mathcal{B}(K_S^0 \to \text{invisible}) \times \varepsilon_{\text{signal}}, \tag{3.2}$$

respectively. Here, $N_{J/\psi \to \phi K_S^0 K_S^0}$ represents the product of the total number of J/ψ events and the BF of $J/\psi \to \phi K_S^0 K_S^0$, while $\mathcal{B}(\phi \to K^+ K^-)$ and $\mathcal{B}(K_S^0 \to \pi^+ \pi^-)$ are the BFs of $\phi \to K^+ K^-$ and $K_S^0 \to \pi^+ \pi^-$ quoted from the PDG [17], respectively. The term $1 - \mathcal{B}(K_S^0 \to \pi^+ \pi^-)$ stands for the probability that K_S^0 decays to processes other than $\pi^+ \pi^-$, which corresponds to our definition of the normalization sample. The efficiencies of selecting the normalization sample and the signal event are denoted by $\varepsilon_{\text{norm.}}$ and $\varepsilon_{\text{signal}}$, respectively.

The BF of the $K_S^0 \to \text{invisible decay is determined as:}$

$$\mathcal{B}(K_S^0 \to \text{ invisible}) = \frac{N_{\text{signal}}}{N_{\text{norm.}}(\varepsilon_{\text{signal}}/\varepsilon_{\text{norm.}})} (1 - \mathcal{B}(K_S^0 \to \pi^+ \pi^-)).$$
 (3.3)

In this approach, the systematic uncertainties arising from the total number of J/ψ events, the BFs of $J/\psi \to \phi K_S^0 K_S^0$ and $\phi \to K^+ K^-$ cancel, and that from the reconstruction efficiencies mostly cancels. To avoid a possible bias, a semi-blind analysis is conducted using a randomly selected 10% subset of the full data sample to validate the analysis strategy. The results presented herein are derived from the full data sample, with the analysis method predetermined and fixed from the 10% sample.

4 Event selection and data analysis

To select the candidates for the normalization sample, where $J/\psi \to \phi K_S^0 K_S^0$, $\phi \to K^+ K^-$, and only one K_S^0 decays to $\pi^+\pi^-$, we reconstruct the events with exactly four charged tracks, ensuring that no additional charged track is present. Charged tracks detected in the MDC are required to be within a polar angle (θ) range of $|\cos\theta| < 0.93$, where θ is defined with respect to the z axis, which is the symmetry axis of the MDC. For charged tracks originating from ϕ decays, the distance of the closest approach to the interaction point (IP), $|V_z|$, must be less than 10 cm along the z axis and less than 1 cm in the plane perpendicular to the z axis. Particle identification (PID) for charged tracks is implemented by combining measurements of the dE/dx in the MDC and the flight time in the TOF to form likelihoods $\mathcal{L}(h), h = K, \pi$, for each hadron h hypothesis. Charged tracks are identified as kaons by requiring $\mathcal{L}(K) > \mathcal{L}(\pi)$. The ϕ meson is reconstructed through the decay $\phi \to K^+K^-$, and its invariant mass, $M(K^+K^-)$, is required to be in the range of $[1.00, 1.04] \, \text{GeV}/c^2$.

The $K_S^0(\text{tag})$ candidates are reconstructed using two oppositely charged tracks, which are each required to satisfy $|V_z| < 20\,\text{cm}$. Tracks are then identified as pions by requiring $\mathcal{L}(\pi) > \mathcal{L}(K)$. A vertex fit constraints the $\pi^+\pi^-$ pairs are constrained to originate from a common vertex. A further fit then constrains the momentum of the $K_S^0(\text{tag})$ candidate to point from the IP to the decay vertex. The measured decay length of the $K_S^0(\text{tag})$ candidate ranges from 0 to 20 cm, following an exponential distribution convolved with the resolution. The ratio of decay length of the $K_S^0(\text{tag})$ candidate to its uncertainty is required to be greater than two, which maintains an efficiency of approximately 90% while effectively suppressing the $\pi^+\pi^-$ combinatorial backgrounds. The signal region for the $\pi^+\pi^-$ invariant mass is $0.486\,\text{GeV}/c^2 < M(\pi^+\pi^-) < 0.510\,\text{GeV}/c^2$.

To further suppress the background from $J/\psi \to \gamma\phi\phi$, $\phi \to K^+K^-$, $\phi \to K_S^0K_L^0$, the recoil mass of the selected ϕ candidate is required to be greater than 1.08 GeV/ c^2 , rendering the contribution from $J/\psi \to \gamma\phi\phi$ negligible. In addition, we require the cosine of the polar angle of the $\phi K_S^0(\text{tag})$ system to be within the interval [-0.80, 0.80]. This condition ensures most of the decay products of the recoiling K_S^0 fall within the acceptance region of the barrel EMC, while a tiny fraction of daughter pions (<4%) may fall outside the acceptance due to their wider angular distribution. Furthermore, the recoil mass of the selected $\phi K_S^0(\text{tag})$ candidate must be within 40 MeV/ c^2 of the known K_S^0 mass [17].

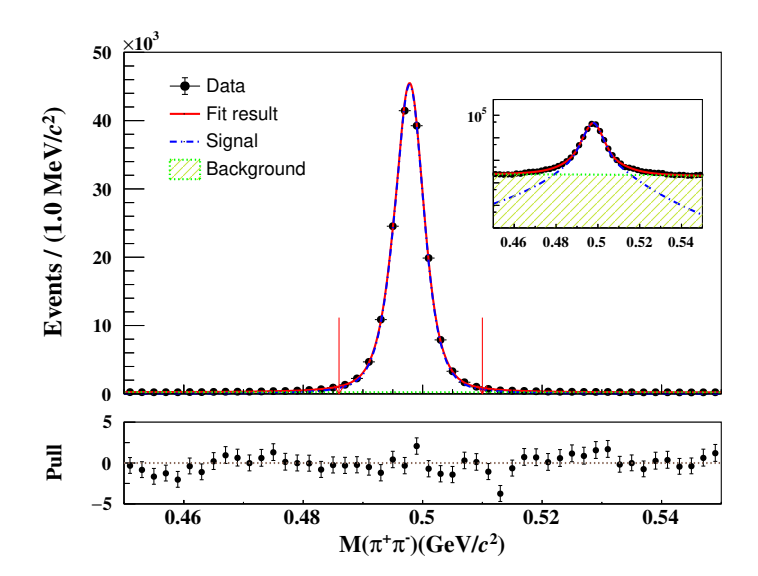


Figure 1. Fit to the distribution of $M(\pi^+\pi^-)$. The black dots with error bars represent data and the red solid line shows the total fit. The blue curve and green dashed area are the fitted signal and non-peaking background shapes, respectively. Note that the green dashed area does not include the four-pion and non- ϕ backgrounds. The red arrows denote the K_S^0 signal region. The inset of the figure displays the fit result with a logarithmic vertical scale. The bottom panel shows the fit residuals.

After applying all the above selection requirements, the analysis of the J/ψ inclusive MC sample indicates that the primary backgrounds sources affecting $N_{\text{norm.}}$ can be categorized into two types: the four-pion and non- ϕ background, with the latter dominant. The four-pion background primarily originates from $J/\psi \to \phi K_S^0 K_S^0$, with both K_S^0 mesons decaying to $\pi^+\pi^-$. The expected yield of the four-pion background in data, as estimated from MC simulation and normalized to the full data sample, is 1022 ± 260 . The non- ϕ background is from $J/\psi \to K^+K^-K_S^0(\text{tag})K_L^0$ and $J/\psi \to K^+K^-K_S^0(\text{tag})K_S^0$. While the contribution from the latter decay can be estimated using MC simulation, the contribution from $J/\psi \to K^+K^-K_S^0(\text{tag})K_L^0$ remains uncertain because its BF has not been measured. Therefore, at this stage, we are unable to directly estimate the contribution from the non- ϕ background. Details about the estimation of this contribution will be discussed in section 5.

To extract the yield of the normalization sample, a binned maximum likelihood fit is performed on the distribution of $M(\pi^+\pi^-)$, as depicted in figure 1. In the fit, the signal is modeled using a double Gaussian function, while the non-peaking background is described by a second-order Chebyshev function. The yield N is determined to be $(1.535 \pm 0.004) \times 10^5$ by integrating the signal function over the K_S^0 signal region. It is noted that N represents a preliminary yield. Given that the four-pion and non- ϕ background peak in the signal region of the $M(\pi^+\pi^-)$ distribution, it is necessary to subtract these contributions from N to obtain the final yield of the normalization sample, N_{norm} .

The efficiency of selecting the normalization sample is determined from a MC sample of $J/\psi \to \phi K_S^0 K_S^0$, with $\phi \to K^+ K^-$ and $K_S^0 \to$ inclusive. For this MC sample, the efficiency is obtained by counting the number of events that survive the selection criteria, and truth information is employed to identify the events where only one K_S^0 decays to $\pi^+\pi^-$. To

improve the modeling of intermediate resonance contributions to $J/\psi \to \phi K_S^0 K_S^0$, the MC events are corrected based on a multidimensional re-weighting method as described in ref. [41]. A clean control sample of $J/\psi \to \phi K_S^0 K_S^0$, with $\phi \to K^+ K^-$ and both K_S^0 mesons decaying to $\pi^+\pi^-$, is selected using the selection criteria similar to that of ref. [42]. Correction factors are derived from this control sample as a function of the invariant masses of $K_S^0 K_S^0$ and ϕK_S^0 , as well as the cosines of the polar angles for the ϕ and K_S^0 , denoted as $\cos \phi$ and $\cos K_S^0$. These correction factors are subsequently applied to the MC samples to correct the MC-simulated shapes, thus enabling accurate determination of the detection efficiencies for both normalization and signal events. The efficiency is determined to be $\varepsilon_{\text{norm.}} = (16.02 \pm 0.06)\%$, where the uncertainty comes from MC statistics. Note the efficiencies do not include the BFs of ϕ and K_S^0 subsequent decays.

We search for the $K_S^0 \to \text{invisible signal using the same selection criteria as those used for selecting the normalization sample. The detection efficiency <math>\varepsilon_{\text{signal}}$ is determined to be $(17.14 \pm 0.04)\%$ based on the signal MC sample of $J/\psi \to \phi K_S^0(\text{tag})K_S^0$, $K_S^0 \to \text{invisible}$. As the K_S^0 invisible decay does not deposit any energy in the EMC, the sum of energies of all EMC showers not associated with any charged tracks, E_{EMC} , can be used to distinguish the signal from background. For the selected showers, we require that they are separated by more than 10° from other charged tracks, and the difference between the EMC time and the event start time is required to be within 700 ns. These requirements remove charged-particle showers and help suppress electronic noise and showers unrelated to the event.

5 Background analysis

The dominant backgrounds affecting the signal side yield, N_{signal} , arise from the following three sources:

- $K_S^0 \to \text{anything background}$, which comes from $J/\psi \to \phi K_S^0(\text{tag})K_S^0$, with K_S^0 decaying to visible particles, such as $K_S^0 \to \pi^0\pi^0$ and $K_S^0 \to \pi^+\pi^-$. Notably, the background from K_S^0 decaying to charged particles, like $K_S^0 \to \pi^+\pi^-$, is strongly suppressed by the selection requirements for four-charged tracks and are thus negligible compared to $K_S^0 \to \pi^0\pi^0$. Consequently, the energy deposited in the EMC $(E_{\rm EMC})$ of $K_S^0 \to \text{anything}$ background is primarily studied using the control sample of $J/\psi \to \phi K_S^0(\text{tag})K_S^0$, $K_S^0 \to \pi^0\pi^0$. Good consistency in the $E_{\rm EMC}$ distributions between data and MC simulation allows us to model the $K_S^0 \to \text{anything}$ background using the MC-simulated shape based on the $K_S^0 \to \pi^0\pi^0$ control sample.
- Non- ϕ background, which originates from $J/\psi \to K^+K^-K_S^0(\text{tag})K_S^0$ and $J/\psi \to K^+K^-K_S^0(\text{tag})K_L^0$. The E_{EMC} of the non- ϕ background is characterized by that of the sideband region of $M(K^+K^-)$ in data, defined as $1.10\,\text{GeV}/c^2 < M(K^+K^-) < 1.14\,\text{GeV}/c^2$. The shape remains stable when using alternative sideband region, and the impact of the sideband choice will be considered as a source of systematic uncertainty.
- Other backgrounds, which arise from J/ψ decays, such as $J/\psi \to \pi^+\pi^-\eta K^+K^-$, and from the continuum process, i.e, $e^+e^- \to \phi K_S^0K_S^0$. The former is studied based on the inclusive MC sample, while the latter is assessed with continuum data collected at $\sqrt{s} = 3.08 \, \text{GeV}$.

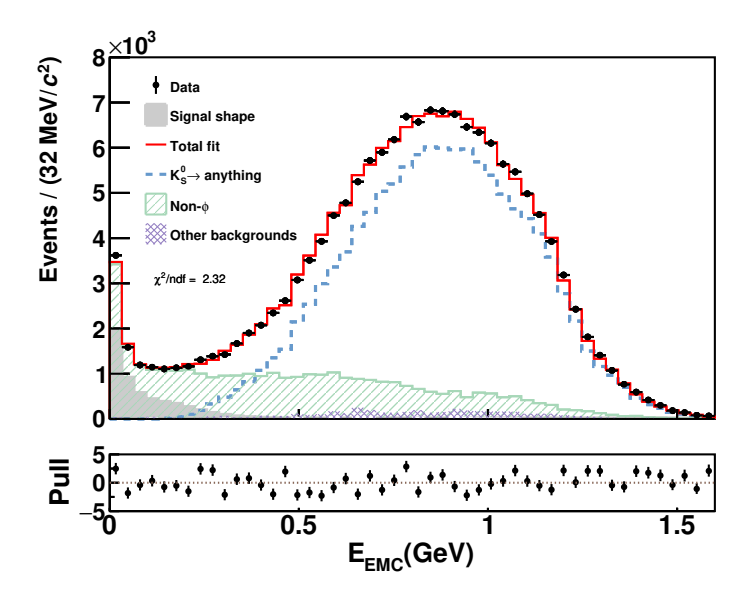


Figure 2. The distributions of $E_{\rm EMC}$ for the accepted candidates in data and the inclusive MC sample. The black dots with error bars are data, the green shaded histogram shows the non- ϕ background, and the purple shaded histogram shows the other backgrounds in inclusive MC sample. The blue line shows the $K_S^0 \to {\rm anything}$ background and the red solid line shows the total fit. The red solid line represents the sum of all the components in the fit, which are stacked together in the plot, while the individual components are shown unstacked. The gray shaded histogram shows the signal shape, normalized to a BF of 8.0×10^{-3} (10x the obtained limit). The bottom panel shows the fit residuals.

The $E_{\rm EMC}$ distribution, as shown in figure 2, demonstrates that the total $E_{\rm EMC}$ distribution from the background model agrees well with the data. A binned maximum likelihood fit is performed to determine the signal yield. In the fit, the signal is described by the MC-simulated shape, which is corrected based on the $K_S^0 \to \pi^+\pi^-$ control sample as detailed in section 4. The yield of the non- ϕ background is a free parameter in the fit, while the total contribution from both non- ϕ and $K_S^0 \to \text{anything backgrounds}$ is fixed to the preliminary yield, N. The continuum background is characterized using the shape derived from the continuum data at $\sqrt{s} = 3.08 \,\text{GeV}$, with a yield normalized to the J/ψ data sample, after taking into account different integrated luminosities and center-of-mass energies [24]. The other backgrounds are modeled using the shape derived from the inclusive MC sample, with a yield normalized to the total number of J/ψ events. No bias is found in the fit procedures through an input/output check using toy MC samples, which are generated by mixing the simulated signal and background events. The fit gives the signal yield $N_{\rm signal}$ to be 56 \pm 201, which is consistent with zero. Additionally, the fit quantifies the contribution from the non- ϕ processes, which allows determination of the final yield for normalization sample by subtracting the identified non- ϕ and four-pion background components from the preliminary yield N. Specifically, the contributions subtracted for the non- ϕ and four-pion backgrounds are $(3.457 \pm 0.049) \times 10^4$ and 1022 ± 260 , respectively. The resulting yield is calculated to be $N_{\text{norm.}} = (1.179 \pm 0.007) \times 10^5$.

Since no significant signal is observed, an UL on the BF of $K_S^0 \to \text{invisible}$ is estimated after taking into account the systematic uncertainties described in the following section.

6 Systematic uncertainties

The strategy of this analysis effectively cancels many potential systematic uncertainties. Specifically, the uncertainties related to the total number of J/ψ events, $\mathcal{B}(J/\psi \to \phi K_S^0 K_S^0)$ and $\mathcal{B}(\phi \to K^+ K^-)$ completely cancel, and those from the selection criteria and the MC model of $J/\psi \to \phi K_S^0 K_S^0$ are greatly reduced by the ratios in eq. (3.3). The remaining systematic uncertainties on $\mathcal{B}(K_S^0 \to \text{invisible})$, as summarized in table 1, are described below.

- $N_{\text{norm.}}$. To estimate the systematic uncertainty in the determination of $N_{\text{norm.}}$, we replace the signal shape of a double Gaussian with a MC-simulated shape convolved with a Gaussian function, and vary the nominal bin size of $1 \text{ MeV}/c^2$ to either $0.5 \text{ MeV}/c^2$ or $2 \text{ MeV}/c^2$. The maximum change in the signal yield, 0.7%, is assigned as the systematic uncertainty.
- BF of $K_S^0 \to \pi^+\pi^-$. The uncertainty of $\mathcal{B}(K_S^0 \to \pi^+\pi^-)$ is 0.1% [17].
- Signal shape. The systematic uncertainty due to the signal shape in the fit to $E_{\rm EMC}$ is evaluated by replacing the nominal signal shape with two alternative models. The first model uses the MC-simulated shapes that are re-weighted following the same procedure as in the nominal analysis. The major difference, however, lies in the derivation of the correction factors, which are now functions of the momentum of K_S^0 and ϕ (denoted as $p_{K_S^0}$ and p_{ϕ}), and the cosine of the corresponding polar angles, $\cos(\phi)$ and $\cos(K_S^0)$. The second model employs the data-driven generator BODY3 [42], which was developed to model contributions from different intermediate states observed in data for a three-body final state. The Dalitz plot from data, corrected for backgrounds and efficiencies, is taken as input for the BODY3 generator.
- $K_S^0 \to anything\ background\ shape$. To account for the uncertainty arising from the background shape of $K_S^0 \to anything$ in the fit to $E_{\rm EMC}$, we employ the same alternative models as used for estimating the uncertainty related to the signal shape.
- Non- ϕ background shape. In order to estimate the systematic uncertainty associated with the background shape of the non- ϕ process, alternative sideband regions, specifically [1.12, 1.16] GeV/ c^2 and [1.08, 1.12] GeV/ c^2 , are taken into consideration.

When estimating the BF of $K_S^0 \to \text{invisible}$, the correlations among different systematic uncertainties are taken into account and varied simultaneously in the likelihood fit.

7 Result

We employ a modified frequentist approach as described in refs. [16, 43, 44], to set the UL of $\mathcal{B}(K_S^0 \to \text{invisible})$ in eq. (3.3) incorporating all the systematic and statistical uncertainties. Thousands of toy samples are generated according to the E_{EMC} distribution observed in data. In each toy sample, the number of events is sampled from a Poisson distribution with a mean value corresponding to the data.

Source	Choice or uncertainty
$N_{ m norm.}$	0.7%
${\cal B}(K^0_S o\pi^+\pi^-)$	0.1%
Signal shape	$\mathcal{W}(p_{K_S^0}, p_{\phi}, \cos \phi, \cos K_S^0), \text{ BODY3 MC}$
$K_S^0 \to \text{anything background shape}$	$\mathcal{W}(p_{K_S^0}, p_{\phi}, \cos \phi, \cos K_S^0), \text{ BODY3 MC}$
Non- ϕ background shape	$[1.12, 1.16], [1.08, 1.12] \mathrm{GeV}/c^2$

Table 1. The systematic uncertainties in setting the UL of $\mathcal{B}(K_S^0 \to \text{invisible})$. The nominal analysis criteria are also included as a choice for the last three rows, but are omitted here to save space.

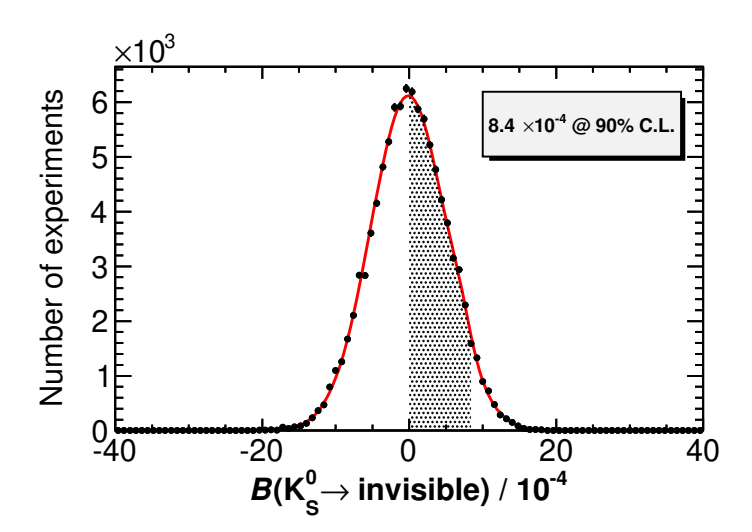


Figure 3. The distribution of $\mathcal{B}(K_S^0 \to \text{invisible})$ determined from toy MC samples. The shaded area corresponds to the 90% coverage in the physical region.

For each toy sample, the same fit procedure used for data is performed, where different systematic uncertainties are randomly varied. The shapes of signal and backgrounds, as listed in table 1, are randomly selected during the fit process. The total contributions from non- ϕ and $K_S^0 \to$ anything are fixed to the values constrained by a Gaussian distribution, with the central value of N, and the uncertainty corresponding to the standard deviation. The uncertainties related to the continuum process and the other background are found to be negligible. To calculate $\mathcal{B}(K_S^0 \to \text{invisible})$ in eq. (3.3), the $\varepsilon_{\text{norm.}}$ and $\varepsilon_{\text{signal}}$ are Gaussian-constrained by their respective statistical uncertainties. $N_{\text{norm.}}$ is also Gaussian-constrained, with widths obtained by the quadrature of the statistical and systematic uncertainties, as detailed in table 1.

The resulting distribution of the calculated $\mathcal{B}(K_S^0 \to \text{invisible})$ across these toy samples is shown in figure 3, which follows a Gaussian distribution as expected. By integrating the Gaussian distribution in the physical region greater than zero, the UL of $\mathcal{B}(K_S^0 \to \text{invisible})$ is determined to be 8.4×10^{-4} at the 90% confidence level.

8 Summary

Based on $(1.0087 \pm 0.0044) \times 10^{10} \ J/\psi$ events collected with the BESIII detector, we search for K_S^0 invisible decays for the first time. No significant signal is observed. The UL on the decay BF is set to be 8.4×10^{-4} at the 90% confidence level. This work provides the first direct measurement of the BF of $K_S^0 \rightarrow$ invisible, with results that are compatible with the indirect estimation. This search also provides a direct experimental basis to perform CPT tests with the BSR without assumptions about invisible decay modes.

Acknowledgments

The BESIII Collaboration thanks the staff of BEPCII and the IHEP computing center for their strong support. This work is supported in part by National Key R&D Program of China under Contracts Nos. 2020YFA0406400, 2023YFA1606000, 2020YFA0406300; Joint Large-Scale Scientific Facility Funds of the NSFC and CAS under Contract No. U1832207; National Natural Science Foundation of China (NSFC) under Contracts Nos. 11635010, 11735014, 11935015, 11935016, 11935018, 12025502, 12035009, 12035013, 12061131003, 12192260, 12192261,12192262, 12192263, 12192264, 12192265, 12221005, 12225509, 12235017, 12361141819; the CAS Large-Scale Scientific Facility Program; the CAS Center for Excellence in Particle Physics (CCEPP); 100 Talents Program of CAS; The Institute of Nuclear and Particle Physics (INPAC) and Shanghai Key Laboratory for Particle Physics and Cosmology; German Research Foundation DFG under Contracts Nos. FOR5327, GRK 2149; Istituto Nazionale di Fisica Nucleare, Italy; Knut and Alice Wallenberg Foundation under Contracts Nos. 2021.0174, 2021.0299; Ministry of Development of Turkey under Contract No. DPT2006K-120470; National Research Foundation of Korea under Contract No. NRF-2022R1A2C1092335; National Science and Technology fund of Mongolia; National Science Research and Innovation Fund (NSRF) via the Program Management Unit for Human Resources & Institutional Development, Research and Innovation of Thailand under Contracts Nos. B16F640076, B50G670107; Polish National Science Centre under Contract No. 2019/35/O/ST2/02907; Swedish Research Council under Contract No. 2019.04595; The Swedish Foundation for International Cooperation in Research and Higher Education under Contract No. CH2018-7756; U.S. Department of Energy under Contract No. DE-FG02-05ER41374.

Data Availability Statement. This article has no associated data or the data will not be deposited.

Code Availability Statement. This article has no associated code or the code will not be deposited.

Open Access. This article is distributed under the terms of the Creative Commons Attribution License (CC-BY4.0), which permits any use, distribution and reproduction in any medium, provided the original author(s) and source are credited.

References

- [1] Planck collaboration, Planck 2018 results. VI. Cosmological parameters, Astron. Astrophys. 641 (2020) A6 [Erratum ibid. 652 (2021) C4] [arXiv:1807.06209] [INSPIRE].
- [2] G. Bertone, D. Hooper and J. Silk, *Particle dark matter: Evidence, candidates and constraints*, *Phys. Rept.* **405** (2005) 279 [hep-ph/0404175] [INSPIRE].
- [3] K.G. Begeman, A.H. Broeils and R.H. Sanders, Extended rotation curves of spiral galaxies: Dark haloes and modified dynamics, Mon. Not. Roy. Astron. Soc. 249 (1991) 523 [INSPIRE].
- [4] G. Lanfranchi, M. Pospelov and P. Schuster, The Search for Feebly Interacting Particles, Ann. Rev. Nucl. Part. Sci. 71 (2021) 279 [arXiv:2011.02157] [INSPIRE].
- [5] E. Goudzovski et al., New physics searches at kaon and hyperon factories, Rept. Prog. Phys. 86 (2023) 016201 [arXiv:2201.07805] [INSPIRE].
- [6] BABAR collaboration, Search for Invisible Decays of the $\Upsilon(1S)$, Phys. Rev. Lett. 103 (2009) 251801 [arXiv:0908.2840] [INSPIRE].
- [7] BES collaboration, Search for the Invisible Decay of J/ψ in $\psi(2S) \to \pi^+\pi^- J/\psi$, Phys. Rev. Lett. 100 (2008) 192001 [arXiv:0710.0039] [INSPIRE].
- [8] Belle collaboration, Search for B⁰ decays to invisible final states, Phys. Rev. D 86 (2012) 032002 [arXiv:1206.5948] [INSPIRE].
- [9] G. Alonso-Álvarez and M. Escudero Abenza, The first limit on invisible decays of B_s mesons comes from LEP, Eur. Phys. J. C 84 (2024) 553 [arXiv:2310.13043] [INSPIRE].
- [10] BESIII collaboration, Search for η and η' invisible decays in $J/\psi \to \phi \eta$ and $J/\psi \to \phi \eta'$, Phys. Rev. D 87 (2013) 012009 [arXiv:1209.2469] [INSPIRE].
- [11] BES collaboration, Search for Invisible Decays of η and η' in $J/\psi \to \phi \eta$ and $\phi \eta'$, Phys. Rev. Lett. **97** (2006) 202002 [hep-ex/0607006] [INSPIRE].
- [12] NA64 collaboration, Dark-Sector Search via Pion-Produced η and η' Mesons Decaying Invisibly in the NA64h Detector, Phys. Rev. Lett. 133 (2024) 121803 [arXiv:2406.01990] [INSPIRE].
- [13] NA62 collaboration, Search for π^0 decays to invisible particles, JHEP **02** (2021) 201 [arXiv:2010.07644] [INSPIRE].
- [14] Belle collaboration, Search for D⁰ decays to invisible final states at Belle, Phys. Rev. D 95 (2017) 011102 [arXiv:1611.09455] [INSPIRE].
- [15] BESIII collaboration, Search for invisible decays of ω and ϕ with J/ψ data at BESIII, Phys. Rev. D 98 (2018) 032001 [arXiv:1805.05613] [INSPIRE].
- [16] BESIII collaboration, Search for invisible decays of the Λ baryon, Phys. Rev. D 105 (2022) L071101 [arXiv:2110.06759] [INSPIRE].
- [17] Particle Data Group collaboration, Review of particle physics, Phys. Rev. D 110 (2024) 030001 [INSPIRE].
- [18] S.N. Gninenko, Search for invisible decays of π^0 , η , η' , K_S and K_L : A probe of new physics and tests using the Bell-Steinberger relation, Phys. Rev. D **91** (2015) 015004 [arXiv:1409.2288] [INSPIRE].
- [19] W. Tan, Invisible decays of neutral hadrons, arXiv:2006.10746 [INSPIRE].
- [20] R.N. Mohapatra, Dark Matter and Mirror World, Entropy 26 (2024) 282 [INSPIRE].

- [21] C.-Q. Geng and J. Tandean, Probing new physics with the kaon decays $K \to \pi\pi E$, Phys. Rev. D 102 (2020) 115021 [arXiv:2009.00608] [INSPIRE].
- [22] KLOE collaboration, Determination of CP and CPT violation parameters in the neutral kaon system using the Bell-Steinberger relation and data from the KLOE experiment, JHEP 12 (2006) 011 [hep-ex/0610034] [INSPIRE].
- [23] J.S. Bell and J. Steinberger, Weak interactions of kaons, in the proceedings of the Oxford International Conference on Elementary Particles, Oxford, U.K., 19–25 September 1966, p. 19–222 [INSPIRE].
- [24] BESIII collaboration, Number of J/ψ events at BESIII, Chin. Phys. C 46 (2022) 074001 [arXiv:2111.07571] [INSPIRE].
- [25] BESIII collaboration, Design and Construction of the BESIII Detector, Nucl. Instrum. Meth. A 614 (2010) 345 [arXiv:0911.4960] [INSPIRE].
- [26] C. Yu et al., BEPCII Performance and Beam Dynamics Studies on Luminosity, in the proceedings of the 7th International Particle Accelerator Conference, Busan, Republic of Korea, 08–13 May 2016 [DOI:10.18429/JACOW-IPAC2016-TUYA01] [INSPIRE].
- [27] BESIII collaboration, Future Physics Programme of BESIII, Chin. Phys. C 44 (2020) 040001 [arXiv:1912.05983] [INSPIRE].
- [28] X. Li et al., Study of MRPC technology for BESIII endcap-TOF upgrade, Radiat. Detect. Technol. Methods 1 (2017) 13 [INSPIRE].
- [29] Y.-X. Guo et al., The study of time calibration for upgraded end cap TOF of BESIII, Radiat. Detect. Technol. Methods 1 (2017) 15 [INSPIRE].
- [30] GEANT4 collaboration, GEANT4: a simulation toolkit, Nucl. Instrum. Meth. A 506 (2003) 250 [INSPIRE].
- [31] M. Ya-Jun, L. Yu-Tie and Y. Zheng-Yun, A method for detector description exchange among ROOT GEANT4 and GEANT3, Chin. Phys. C 32 (2008) 572 [INSPIRE].
- [32] Y.-T. Liang et al., A uniform geometry description for simulation, reconstruction and visualization in the BESIII experiment, Nucl. Instrum. Meth. A 603 (2009) 325 [INSPIRE].
- [33] K.-X. Huang et al., Method for detector description transformation to Unity and application in BESIII, Nucl. Sci. Tech. 33 (2022) 142 [arXiv:2206.10117] [INSPIRE].
- [34] S. Jadach, B.F.L. Ward and Z. Was, Coherent exclusive exponentiation for precision Monte Carlo calculations, Phys. Rev. D 63 (2001) 113009 [hep-ph/0006359] [INSPIRE].
- [35] S. Jadach, B.F.L. Ward and Z. Was, The precision Monte Carlo event generator K K for two fermion final states in e⁺e⁻ collisions, Comput. Phys. Commun. 130 (2000) 260 [hep-ph/9912214] [INSPIRE].
- [36] D.J. Lange, The EvtGen particle decay simulation package, Nucl. Instrum. Meth. A 462 (2001) 152 [INSPIRE].
- [37] R.-G. Ping, Event generators at BESIII, Chin. Phys. C 32 (2008) 599 [INSPIRE].
- [38] J.C. Chen et al., Event generator for J/ψ and $\psi(2S)$ decay, Phys. Rev. D **62** (2000) 034003 [INSPIRE].
- [39] R.-L. Yang, R.-G. Ping and H. Chen, Tuning and Validation of the Lundcharm Model with J/ψ Decays, Chin. Phys. Lett. **31** (2014) 061301 [INSPIRE].

- [40] E. Richter-Was, QED bremsstrahlung in semileptonic B and leptonic tau decays, Phys. Lett. B 303 (1993) 163 [INSPIRE].
- [41] A. Rogozhnikov, Reweighting with Boosted Decision Trees, J. Phys. Conf. Ser. 762 (2016) 012036 [arXiv:1608.05806] [INSPIRE].
- [42] BESIII collaboration, Measurement of the branching fraction for the decay $\psi(3686) \rightarrow \phi K_S^0 K_S^0$, Phys. Rev. D 108 (2023) 052001 [arXiv:2303.08317] [INSPIRE].
- [43] BESIII collaboration, Search for the radiative leptonic decay $D^+ \to \gamma e^+ \nu_e$, Phys. Rev. D 95 (2017) 071102 [arXiv:1702.05837] [INSPIRE].
- [44] BESIII collaboration, Search for the decay $D^0 \to \pi^0 \nu \bar{\nu}$, Phys. Rev. D **105** (2022) L071102 [arXiv:2112.14236] [INSPIRE].

The BESIII collaboration

```
M. Ablikim<sup>1</sup>, M.N. Achasov<sup>4,c</sup>, P. Adlarson<sup>76</sup>, O. Afedulidis<sup>3</sup>, X.C. Ai<sup>81</sup>, R. Aliberti<sup>35</sup>,
A. Amoroso<sup>75A,75C</sup>, Q. An<sup>72,58,a</sup>, Y. Bai<sup>57</sup>, O. Bakina<sup>36</sup>, I. Balossino<sup>29A</sup>, Y. Ban<sup>46,h</sup>, H.-R. Bao<sup>64</sup>,
V. Batozskaya<sup>1,44</sup>, K. Begzsuren<sup>32</sup>, N. Berger<sup>35</sup>, M. Berlowski<sup>44</sup>, M. Bertani<sup>28A</sup>, D. Bettoni<sup>29A</sup>,
F. Bianchi<sup>75A,75C</sup>, E. Bianco<sup>75A,75C</sup>, A. Bortone<sup>75A,75C</sup>, I. Boyko<sup>36</sup>, R.A. Briere<sup>5</sup>, A. Brueggemann<sup>69</sup>,
H. Cai<sup>77</sup>, X. Cai<sup>1,58</sup>, A. Calcaterra<sup>28A</sup>, G.F. Cao<sup>1,64</sup>, N. Cao<sup>1,64</sup>, S.A. Cetin<sup>62A</sup>, X.Y. Chai<sup>46,h</sup>,
J.F. Chang<sup>1,58</sup>, G.R. Che<sup>43</sup>, Y.Z. Che<sup>1,58,64</sup>, G. Chelkov<sup>36,b</sup>, C. Chen<sup>43</sup>, C.H. Chen<sup>9</sup>, Chao Chen<sup>55</sup>,
G. Chen<sup>1</sup>, H.S. Chen<sup>1,64</sup>, H.Y. Chen<sup>20</sup>, M.L. Chen<sup>1,58,64</sup>, S.J. Chen<sup>42</sup>, S.L. Chen<sup>45</sup>, S.M. Chen<sup>61</sup>,
T. Chen<sup>1,64</sup>, X.R. Chen<sup>31,64</sup>, X.T. Chen<sup>1,64</sup>, Y.B. Chen<sup>1,58</sup>, Y.Q. Chen<sup>34</sup>, Z.J. Chen<sup>25,i</sup>, S.K. Choi<sup>10</sup>,
G. Cibinetto<sup>29A</sup>, F. Cossio<sup>75C</sup>, J.J. Cui<sup>50</sup>, H.L. Dai<sup>1,58</sup>, J.P. Dai<sup>79</sup>, A. Dbeyssi<sup>18</sup>, R. E. de Boer<sup>3</sup>,
D. Dedovich<sup>36</sup>, C.Q. Deng<sup>73</sup>, Z.Y. Deng<sup>1</sup>, A. Denig<sup>35</sup>, I. Denysenko<sup>36</sup>, M. Destefanis<sup>75A,75C</sup>,
F. De Mori<sup>75A,75C</sup>, B. Ding<sup>67,1</sup>, X.X. Ding<sup>46,h</sup>, Y. Ding<sup>34</sup>, Y. Ding<sup>40</sup>, J. Dong<sup>1,58</sup>, L.Y. Dong<sup>1,64</sup>,
M.Y. Dong<sup>1,58,64</sup>, X. Dong<sup>77</sup>, M.C. Du<sup>1</sup>, S.X. Du<sup>81</sup>, Y.Y. Duan<sup>55</sup>, Z.H. Duan<sup>42</sup>, P. Egorov<sup>36,b</sup>,
G.F. Fan<sup>42</sup>, J.J. Fan<sup>19</sup>, Y.H. Fan<sup>45</sup>, J. Fang<sup>1,58</sup>, J. Fang<sup>59</sup>, S.S. Fang<sup>1,64</sup>, W.X. Fang<sup>1</sup>, Y.Q. Fang<sup>1,58</sup>,
R. Farinelli<sup>29A</sup>, L. Fava<sup>75B,75C</sup>, F. Feldbauer<sup>3</sup>, G. Felici<sup>28A</sup>, C.Q. Feng<sup>72,58</sup>, J.H. Feng<sup>59</sup>,
Y.T. Feng<sup>72,58</sup>, M. Fritsch<sup>3</sup>, C.D. Fu<sup>1</sup>, J.L. Fu<sup>64</sup>, Y.W. Fu<sup>1,64</sup>, H. Gao<sup>64</sup>, X.B. Gao<sup>41</sup>, Y.N. Gao<sup>19</sup>,
Y.N. Gao<sup>46,h</sup>, Yang Gao<sup>72,58</sup>, S. Garbolino<sup>75C</sup>, I. Garzia<sup>29A,29B</sup>, P.T. Ge<sup>19</sup>, Z.W. Ge<sup>42</sup>, C. Geng<sup>59</sup>,
E.M. Gersabeck<sup>68</sup>, A. Gilman<sup>70</sup>, K. Goetzen<sup>13</sup>, L. Gong<sup>40</sup>, W.X. Gong<sup>1,58</sup>, W. Gradl<sup>35</sup>,
S. Gramigna<sup>29A,29B</sup>, M. Greco<sup>75A,75C</sup>, M.H. Gu<sup>1,58</sup>, Y.T. Gu<sup>15</sup>, C.Y. Guan<sup>1,64</sup>, A.Q. Guo<sup>31,64</sup>,
L.B. Guo<sup>41</sup>, M.J. Guo<sup>50</sup>, R.P. Guo<sup>49</sup>, Y.P. Guo<sup>12,g</sup>, A. Guskov<sup>36,b</sup>, J. Gutierrez<sup>27</sup>, K.L. Han<sup>64</sup>,
T.T. Han<sup>1</sup>, F. Hanisch<sup>3</sup>, X.Q. Hao<sup>19</sup>, F.A. Harris<sup>66</sup>, K.K. He<sup>55</sup>, K.L. He<sup>1,64</sup>, F.H. Heinsius<sup>3</sup>,
C.H. Heinz<sup>35</sup>, Y.K. Heng<sup>1,58,64</sup>, C. Herold<sup>60</sup>, T. Holtmann<sup>3</sup>, P.C. Hong<sup>34</sup>, G.Y. Hou<sup>1,64</sup>, X.T. Hou<sup>1,64</sup>,
 \text{Y.R. Hou}^{64}, \, \text{Z.L. Hou}^{1}, \, \text{B.Y. Hu}^{59}, \, \text{H.M. Hu}^{1,64}, \, \text{J.F. Hu}^{56,j}, \, \text{Q.P. Hu}^{72,58}, \, \text{S.L. Hu}^{12,g}, \, \text{T. Hu}^{1,58,64}, \, \text{H.M. Hu}^{1,64}, \, \text{J.F. Hu
Y. Hu<sup>1</sup>, G.S. Huang<sup>72,58</sup>, K.X. Huang<sup>59</sup>, L.Q. Huang<sup>31,64</sup>, P. Huang<sup>42</sup>, X.T. Huang<sup>50</sup>, Y.P. Huang<sup>1</sup>,
Y.S. Huang<sup>59</sup>, T. Hussain<sup>74</sup>, F. Hölzken<sup>3</sup>, N. Hüsken<sup>35</sup>, N. in der Wiesche<sup>69</sup>, J. Jackson<sup>27</sup>,
S. Janchiv^{32}, Q. Ji^1, Q.P. Ji^{19}, W. Ji^{1,64}, X.B. Ji^{1,64}, X.L. Ji^{1,58}, Y.Y. Ji^{50}, X.Q. Jia^{50}, Z.K. Jia^{72,58},
D. Jiang<sup>1,64</sup>, H.B. Jiang<sup>77</sup>, P.C. Jiang<sup>46,h</sup>, S.S. Jiang<sup>39</sup>, T.J. Jiang<sup>16</sup>, X.S. Jiang<sup>1,58,64</sup>, Y. Jiang<sup>64</sup>,
J.B. Jiao<sup>50</sup>, J.K. Jiao<sup>34</sup>, Z. Jiao<sup>23</sup>, S. Jin<sup>42</sup>, Y. Jin<sup>67</sup>, M.Q. Jing<sup>1,64</sup>, X.M. Jing<sup>64</sup>, T. Johansson<sup>76</sup>,
S. Kabana<sup>33</sup>, N. Kalantar-Nayestanaki<sup>65</sup>, X.L. Kang<sup>9</sup>, X.S. Kang<sup>40</sup>, M. Kavatsyuk<sup>65</sup>, B.C. Ke<sup>81</sup>,
V. Khachatryan<sup>27</sup>, A. Khoukaz<sup>69</sup>, R. Kiuchi<sup>1</sup>, O.B. Kolcu<sup>62A</sup>, B. Kopf<sup>3</sup>, M. Kuessner<sup>3</sup>, X. Kui<sup>1,64</sup>,
N. Kumar<sup>26</sup>, A. Kupsc<sup>44,76</sup>, W. Kühn<sup>37</sup>, W.N. Lan<sup>19</sup>, T.T. Lei<sup>72,58</sup>, Z.H. Lei<sup>72,58</sup>, M. Lellmann<sup>35</sup>,
T. Lenz<sup>35</sup>, C. Li<sup>47</sup>, C. Li<sup>43</sup>, C.H. Li<sup>39</sup>, Cheng Li<sup>72,58</sup>, D.M. Li<sup>81</sup>, F. Li<sup>1,58</sup>, G. Li<sup>1</sup>, H.B. Li<sup>1,64</sup>,
H.J. Li^{19}, H.N. Li^{56,j}, Hui Li^{43}, J.R. Li^{61}, J.S. Li^{59}, K. Li^{1}, K.L. Li^{19}, L.J. Li^{1,64}, Lei Li^{48}, M.H. Li^{43},
P.L. \text{Li}^{64}, P.R. \text{Li}^{38,k,l}, Q.M. \text{Li}^{1,64}, Q.X. \text{Li}^{50}, R. \text{Li}^{17,31}, T. \text{Li}^{50}, T.Y. \text{Li}^{43}, W.D. \text{Li}^{1,64}, W.G. \text{Li}^{1,a},
X. Li<sup>1,64</sup>, X.H. Li<sup>72,58</sup>, X.L. Li<sup>50</sup>, X.Y. Li<sup>1,8</sup>, X.Z. Li<sup>59</sup>, Y. Li<sup>19</sup>, Y.G. Li<sup>46,h</sup>, Z.J. Li<sup>59</sup>, Z.Y. Li<sup>79</sup>,
C. Liang<sup>42</sup>, H. Liang<sup>72,58</sup>, Y.F. Liang<sup>54</sup>, Y.T. Liang<sup>31,64</sup>, G.R. Liao<sup>14</sup>, Y.P. Liao<sup>1,64</sup>, J. Libby<sup>26</sup>,
A. Limphirat<sup>60</sup>, C.C. Lin<sup>55</sup>, C.X. Lin<sup>64</sup>, D.X. Lin<sup>31,64</sup>, T. Lin<sup>1</sup>, B.J. Liu<sup>1</sup>, B.X. Liu<sup>77</sup>, C. Liu<sup>34</sup>,
C.X. Liu<sup>1</sup>, F. Liu<sup>1</sup>, F.H. Liu<sup>53</sup>, Feng Liu<sup>6</sup>, G.M. Liu<sup>56,j</sup>, H. Liu<sup>38,k,l</sup>, H.B. Liu<sup>15</sup>, H.H. Liu<sup>1</sup>,
\text{H.M. Liu}^{1,64}, \text{Huihui Liu}^{21}, \text{J.B. Liu}^{72,58}, \text{K. Liu}^{38,k,l}, \text{K.Y. Liu}^{40}, \text{Ke Liu}^{22}, \text{L. Liu}^{72,58}, \text{L.C. Liu}^{43},
Lu Liu<sup>43</sup>, M.H. Liu<sup>12,g</sup>, P.L. Liu<sup>1</sup>, Q. Liu<sup>64</sup>, S.B. Liu<sup>72,58</sup>, T. Liu<sup>12,g</sup>, W.K. Liu<sup>43</sup>, W.M. Liu<sup>72,58</sup>,
X. Liu<sup>38,k,l</sup>, X. Liu<sup>39</sup>, Y. Liu<sup>38,k,l</sup>, Y. Liu<sup>81</sup>, Y.B. Liu<sup>43</sup>, Z.A. Liu<sup>1,58,64</sup>, Z.D. Liu<sup>9</sup>, Z.Q. Liu<sup>50</sup>,
X.C. Lou<sup>1,58,64</sup>, F.X. Lu<sup>59</sup>, H.J. Lu<sup>23</sup>, J.G. Lu<sup>1,58</sup>, Y. Lu<sup>7</sup>, Y.P. Lu<sup>1,58</sup>, Z.H. Lu<sup>1,64</sup>, C.L. Luo<sup>41</sup>,
J.R. Luo<sup>59</sup>, M.X. Luo<sup>80</sup>, T. Luo<sup>12,g</sup>, X.L. Luo<sup>1,58</sup>, X.R. Lyu<sup>64</sup>, Y.F. Lyu<sup>43</sup>, F.C. Ma<sup>40</sup>, H. Ma<sup>79</sup>,
```

```
H.L. Ma<sup>1</sup>, J.L. Ma<sup>1,64</sup>, L.L. Ma<sup>50</sup>, L.R. Ma<sup>67</sup>, Q.M. Ma<sup>1</sup>, R.Q. Ma<sup>1,64</sup>, R.Y. Ma<sup>19</sup>, T. Ma<sup>72,58</sup>,
X.T. Ma<sup>1,64</sup>, X.Y. Ma<sup>1,58</sup>, Y.M. Ma<sup>31</sup>, F.E. Maas<sup>18</sup>, I. MacKay<sup>70</sup>, M. Maggiora<sup>75A,75C</sup>, S. Malde<sup>70</sup>,
Y.J. Mao<sup>46,h</sup>, Z.P. Mao<sup>1</sup>, S. Marcello<sup>75A,75C</sup>, Y.H. Meng<sup>64</sup>, Z.X. Meng<sup>67</sup>, J.G. Messchendorp<sup>13,65</sup>,
G. Mezzadri<sup>29A</sup>, H. Miao<sup>1,64</sup>, T.J. Min<sup>42</sup>, R.E. Mitchell<sup>27</sup>, X.H. Mo<sup>1,58,64</sup>, B. Moses<sup>27</sup>,
N. Yu. Muchnoi<sup>4,c</sup>, J. Muskalla<sup>35</sup>, Y. Nefedov<sup>36</sup>, F. Nerling<sup>18,e</sup>, L.S. Nie<sup>20</sup>, I.B. Nikolaev<sup>4,c</sup>,
Z. Ning<sup>1,58</sup>, S. Nisar<sup>11,m</sup>, Q.L. Niu<sup>38,k,l</sup>, W.D. Niu<sup>55</sup>, Y. Niu <sup>50</sup>, S.L. Olsen<sup>10,64</sup>, Q. Ouyang<sup>1,58,64</sup>,
S. Pacetti<sup>28B,28C</sup>, X. Pan<sup>55</sup>, Y. Pan<sup>57</sup>, A. Pathak<sup>10</sup>, Y.P. Pei<sup>72,58</sup>, M. Pelizaeus<sup>3</sup>, H.P. Peng<sup>72,58</sup>,
Y.Y. Peng<sup>38,k,l</sup>, K. Peters<sup>13,e</sup>, J.L. Ping<sup>41</sup>, R.G. Ping<sup>1,64</sup>, S. Plura<sup>35</sup>, V. Prasad<sup>33</sup>, F.Z. Qi<sup>1</sup>, H.R. Qi<sup>61</sup>,
M. Qi<sup>42</sup>, S. Qian<sup>1,58</sup>, W.B. Qian<sup>64</sup>, C.F. Qiao<sup>64</sup>, J.H. Qiao<sup>19</sup>, J.J. Qin<sup>73</sup>, L.Q. Qin<sup>14</sup>, L.Y. Qin<sup>72,58</sup>,
X.P. Qin<sup>12,g</sup>, X.S. Qin<sup>50</sup>, Z.H. Qin<sup>1,58</sup>, J.F. Qiu<sup>1</sup>, Z.H. Qu<sup>73</sup>, C.F. Redmer<sup>35</sup>, K.J. Ren<sup>39</sup>,
A. Rivetti<sup>75C</sup>, M. Rolo<sup>75C</sup>, G. Rong<sup>1,64</sup>, Ch. Rosner<sup>18</sup>, M.Q. Ruan<sup>1,58</sup>, S.N. Ruan<sup>43</sup>, N. Salone<sup>44</sup>,
A. Sarantsev<sup>36,d</sup>, Y. Schelhaas<sup>35</sup>, K. Schoenning<sup>76</sup>, M. Scodeggio<sup>29A</sup>, K.Y. Shan<sup>12,g</sup>, W. Shan<sup>24</sup>,
X.Y. Shan<sup>72,58</sup>, Z.J. Shang<sup>38,k,l</sup>, J.F. Shangguan<sup>16</sup>, L.G. Shao<sup>1,64</sup>, M. Shao<sup>72,58</sup>, C.P. Shen<sup>12,g</sup>,
H.F. Shen<sup>1,8</sup>, W.H. Shen<sup>64</sup>, X.Y. Shen<sup>1,64</sup>, B.A. Shi<sup>64</sup>, H. Shi<sup>72,58</sup>, J.L. Shi<sup>12,9</sup>, J.Y. Shi<sup>1</sup>, S.Y. Shi<sup>73</sup>,
X. \text{Shi}^{1,58}, J.J. \text{Song}^{19}, T.Z. \text{Song}^{59}, W.M. \text{Song}^{34,1}, Y. J. \text{Song}^{12,g}, Y.X. \text{Song}^{46,h,n}, S. \text{Sosio}^{75A,75C},
S. Spataro<sup>75A,75C</sup>, F. Stieler<sup>35</sup>, S. S Su<sup>40</sup>, Y.J. Su<sup>64</sup>, G.B. Sun<sup>77</sup>, G.X. Sun<sup>1</sup>, H. Sun<sup>64</sup>, H.K. Sun<sup>1</sup>,
J.F. Sun<sup>19</sup>, K. Sun<sup>61</sup>, L. Sun<sup>77</sup>, S.S. Sun<sup>1,64</sup>, T. Sun<sup>51,f</sup>, Y.J. Sun<sup>72,58</sup>, Y.Z. Sun<sup>1</sup>, Z.Q. Sun<sup>1,64</sup>,
Z.T. Sun<sup>50</sup>, C.J. Tang<sup>54</sup>, G.Y. Tang<sup>1</sup>, J. Tang<sup>59</sup>, M. Tang<sup>72,58</sup>, Y.A. Tang<sup>77</sup>, L.Y. Tao<sup>73</sup>, M. Tat<sup>70</sup>,
J.X. Teng<sup>72,58</sup>, V. Thoren<sup>76</sup>, W.H. Tian<sup>59</sup>, Y. Tian<sup>31,64</sup>, Z.F. Tian<sup>77</sup>, I. Uman<sup>62B</sup>, Y. Wan<sup>55</sup>,
S.J. Wang<sup>50</sup>, B. Wang<sup>1</sup>, Bo Wang<sup>72,58</sup>, C. Wang<sup>19</sup>, D.Y. Wang<sup>46,h</sup>, H.J. Wang<sup>38,k,l</sup>, J.J. Wang<sup>77</sup>,
J.P. Wang <sup>50</sup>, K. Wang<sup>1,58</sup>, L.L. Wang<sup>1</sup>, L.W. Wang<sup>34</sup>, M. Wang<sup>50</sup>, N.Y. Wang<sup>64</sup>, S. Wang<sup>38,k,l</sup>,
S. Wang<sup>12,g</sup>, T. Wang<sup>12,g</sup>, T.J. Wang<sup>43</sup>, W. Wang<sup>59</sup>, W. Wang<sup>73</sup>, W.P. Wang<sup>35,58,72,o</sup>, X. Wang<sup>46,h</sup>,
X.F. Wang<sup>38,k,l</sup>, X.J. Wang<sup>39</sup>, X.L. Wang<sup>12,g</sup>, X.N. Wang<sup>1</sup>, Y. Wang<sup>61</sup>, Y.D. Wang<sup>45</sup>,
Y.F. Wang<sup>1,58,64</sup>, Y.H. Wang<sup>38,k,l</sup>, Y.L. Wang<sup>19</sup>, Y.N. Wang<sup>45</sup>, Y.Q. Wang<sup>1</sup>, Yaqian Wang<sup>17</sup>,
Yi Wang<sup>61</sup>, Z. Wang<sup>1,58</sup>, Z.L. Wang<sup>73</sup>, Z.Y. Wang<sup>1,64</sup>, D.H. Wei<sup>14</sup>, F. Weidner<sup>69</sup>, S.P. Wen<sup>1</sup>,
Y.R. Wen<sup>39</sup>, U. Wiedner<sup>3</sup>, G. Wilkinson<sup>70</sup>, M. Wolke<sup>76</sup>, L. Wollenberg<sup>3</sup>, C. Wu<sup>39</sup>, J.F. Wu<sup>1,8</sup>,
L.H. Wu^{1}, L.J. Wu^{1,64}, Lianjie Wu^{19}, X. Wu^{12,g}, X.H. Wu^{34}, Y.H. Wu^{55}, Y.J. Wu^{31}, Z. Wu^{1,58},
L. Xia<sup>72,58</sup>, X.M. Xian<sup>39</sup>, B.H. Xiang<sup>1,64</sup>, T. Xiang<sup>46,h</sup>, D. Xiao<sup>38,k,l</sup>, G.Y. Xiao<sup>42</sup>, H. Xiao<sup>73</sup>,
Y. L. Xiao<sup>12,g</sup>, Z.J. Xiao<sup>41</sup>, C. Xie<sup>42</sup>, X.H. Xie<sup>46,h</sup>, Y. Xie<sup>50</sup>, Y.G. Xie<sup>1,58</sup>, Y.H. Xie<sup>6</sup>, Z.P. Xie<sup>72,58</sup>,
T.Y. Xing<sup>1,64</sup>, C.F. Xu<sup>1,64</sup>, C.J. Xu<sup>59</sup>, G.F. Xu<sup>1</sup>, M. Xu<sup>72,58</sup>, Q.J. Xu<sup>16</sup>, Q.N. Xu<sup>30</sup>, W.L. Xu<sup>67</sup>,
X.P. Xu^{55}, Y. Xu^{40}, Y.C. Xu^{78}, Z.S. Xu^{64}, F. Yan^{12,g}, L. Yan^{12,g}, W.B. Yan^{72,58}, W.C. Yan^{81},
W.P. Yan<sup>19</sup>, X.Q. Yan<sup>1,64</sup>, H.J. Yang<sup>51,f</sup>, H.L. Yang<sup>34</sup>, H.X. Yang<sup>1</sup>, J.H. Yang<sup>42</sup>, R.J. Yang<sup>19</sup>,
T. Yang<sup>1</sup>, Y. Yang<sup>12,g</sup>, Y.F. Yang<sup>43</sup>, Y.X. Yang<sup>1,64</sup>, Y.Z. Yang<sup>19</sup>, Z.W. Yang<sup>38,k,l</sup>, Z.P. Yao<sup>50</sup>,
M. Ye<sup>1,58</sup>, M.H. Ye<sup>8</sup>, Junhao Yin<sup>43</sup>, Z.Y. You<sup>59</sup>, B.X. Yu<sup>1,58,64</sup>, C.X. Yu<sup>43</sup>, G. Yu<sup>13</sup>, J.S. Yu<sup>25,i</sup>
M.C. Yu<sup>40</sup>, T. Yu<sup>73</sup>, X.D. Yu<sup>46,h</sup>, C.Z. Yuan<sup>1,64</sup>, J. Yuan<sup>34</sup>, J. Yuan<sup>45</sup>, L. Yuan<sup>2</sup>, S.C. Yuan<sup>1,64</sup>,
Y. Yuan<sup>1,64</sup>, Z.Y. Yuan<sup>59</sup>, C.X. Yue<sup>39</sup>, Ying Yue<sup>19</sup>, A.A. Zafar<sup>74</sup>, F.R. Zeng<sup>50</sup>, S.H. Zeng<sup>63</sup>,
X. Zeng<sup>12,g</sup>, Y. Zeng<sup>25,i</sup>, Y.J. Zeng<sup>59</sup>, Y.J. Zeng<sup>1,64</sup>, X.Y. Zhai<sup>34</sup>, Y.C. Zhai<sup>50</sup>, Y.H. Zhan<sup>59</sup>,
A.Q. Zhang<sup>1,64</sup>, B.L. Zhang<sup>1,64</sup>, B.X. Zhang<sup>1</sup>, D.H. Zhang<sup>43</sup>, G.Y. Zhang<sup>19</sup>, H. Zhang<sup>72,58</sup>,
H. Zhang<sup>81</sup>, H.C. Zhang<sup>1,58,64</sup>, H.H. Zhang<sup>59</sup>, H.Q. Zhang<sup>1,58,64</sup>, H.R. Zhang<sup>72,58</sup>, H.Y. Zhang<sup>1,58</sup>,
J. Zhang<sup>59</sup>, J. Zhang<sup>81</sup>, J.J. Zhang<sup>52</sup>, J.L. Zhang<sup>20</sup>, J.Q. Zhang<sup>41</sup>, J.S. Zhang<sup>12,g</sup>, J.W. Zhang<sup>1,58,64</sup>,
J.X. Zhang<sup>38,k,l</sup>, J.Y. Zhang<sup>1</sup>, J.Z. Zhang<sup>1,64</sup>, Jianyu Zhang<sup>64</sup>, L.M. Zhang<sup>61</sup>, Lei Zhang<sup>42</sup>,
P. Zhang<sup>1,64</sup>, Q. Zhang<sup>19</sup>, Q.Y. Zhang<sup>34</sup>, R.Y. Zhang<sup>38,k,l</sup>, S.H. Zhang<sup>1,64</sup>, Shulei Zhang<sup>25,i</sup>,
X.M. Zhang<sup>1</sup>, X. Y Zhang<sup>40</sup>, X.Y. Zhang<sup>50</sup>, Y. Zhang<sup>1</sup>, Y. Zhang<sup>73</sup>, Y.T. Zhang<sup>81</sup>, Y.H. Zhang<sup>1,58</sup>,
```

- Y.M. Zhang³⁹, Yan Zhang^{72,58}, Z.D. Zhang¹, Z.H. Zhang¹, Z.L. Zhang³⁴, Z.X. Zhang¹⁹, Z.Y. Zhang⁴³, Z.Y. Zhang⁷⁷, Z.Z. Zhang⁴⁵, Zh. Zhang¹⁹, G. Zhao¹, J.Y. Zhao^{1,64}, J.Z. Zhao^{1,58}, L. Zhao¹, Lei Zhao^{72,58}, M.G. Zhao⁴³, N. Zhao⁷⁹, R.P. Zhao⁶⁴, S.J. Zhao⁸¹, Y.B. Zhao^{1,58}, Y.X. Zhao^{31,64}, Z.G. Zhao^{72,58}, A. Zhemchugov^{36,b}, B. Zheng⁷³, B.M. Zheng³⁴, J.P. Zheng^{1,58}, W.J. Zheng^{1,64}, X.R. Zheng¹⁹, Y.H. Zheng⁶⁴, B. Zhong⁴¹, X. Zhong⁵⁹, H. Zhou^{35,50,o}, J.Y. Zhou³⁴, S. Zhou⁶, X. Zhou⁷⁷, X.K. Zhou⁶, X.R. Zhou^{72,58}, X.Y. Zhou³⁹, Y.Z. Zhou^{12,g}, Z.C. Zhou²⁰, A.N. Zhu⁶⁴, J. Zhu⁴³, K. Zhu¹, K.J. Zhu^{1,58,64}, K.S. Zhu^{12,g}, L. Zhu³⁴, L.X. Zhu⁶⁴, S.H. Zhu⁷¹, T.J. Zhu^{12,g}, W.D. Zhu⁴¹, W.J. Zhu¹, W.Z. Zhu¹⁹, Y.C. Zhu^{72,58}, Z.A. Zhu^{1,64}, J.H. Zou¹, J. Zu^{72,58}
 - ¹ Institute of High Energy Physics, Beijing 100049, People's Republic of China
 - ² Beihang University, Beijing 100191, People's Republic of China
 - ³ Bochum Ruhr-University, D-44780 Bochum, Germany
 - ⁴ Budker Institute of Nuclear Physics SB RAS (BINP), Novosibirsk 630090, Russia
 - ⁵ Carnegie Mellon University, Pittsburgh, Pennsylvania 15213, U.S.A.
 - ⁶ Central China Normal University, Wuhan 430079, People's Republic of China
 - ⁷ Central South University, Changsha 410083, People's Republic of China
 - ⁸ China Center of Advanced Science and Technology, Beijing 100190, People's Republic of China
 - ⁹ China University of Geosciences, Wuhan 430074, People's Republic of China
 - 10 Chung-Ang University, Seoul, 06974, Republic of Korea
 - ¹¹ COMSATS University Islamabad, Lahore Campus, Defence Road, Off Raiwind Road, 54000 Lahore, Pakistan
 - ¹² Fudan University, Shanghai 200433, People's Republic of China
 - ¹³ GSI Helmholtzcentre for Heavy Ion Research GmbH, D-64291 Darmstadt, Germany
 - ¹⁴ Guangxi Normal University, Guilin 541004, People's Republic of China
 - ¹⁵ Guangxi University, Nanning 530004, People's Republic of China
 - $^{16}\; Hangzhou\; Normal\; University,\; Hangzhou\; 310036,\; People's\; Republic\; of\; China$
 - ¹⁷ Hebei University, Baoding 071002, People's Republic of China
 - ¹⁸ Helmholtz Institute Mainz, Staudinger Weg 18, D-55099 Mainz, Germany
 - ¹⁹ Henan Normal University, Xinxiang 453007, People's Republic of China
 - ²⁰ Henan University, Kaifeng 475004, People's Republic of China
 - ²¹ Henan University of Science and Technology, Luoyang 471003, People's Republic of China
 - ²² Henan University of Technology, Zhengzhou 450001, People's Republic of China
 - ²³ Huangshan College, Huangshan 245000, People's Republic of China
 - ²⁴ Hunan Normal University, Changsha 410081, People's Republic of China
 - $^{25}\ Hunan\ University,\ Changsha\ 410082,\ People's\ Republic\ of\ China$
 - ²⁶ Indian Institute of Technology Madras, Chennai 600036, India
 - ²⁷ Indiana University, Bloomington, Indiana 47405, U.S.A.
 - ²⁸ INFN Laboratori Nazionali di Frascati, (A) INFN Laboratori Nazionali di Frascati, I-00044, Frascati, Italy; (B) INFN Sezione di Perugia, I-06100, Perugia, Italy; (C) University of Perugia, I-06100, Perugia, Italy
 - ²⁹ INFN Sezione di Ferrara, (A) INFN Sezione di Ferrara, I-44122, Ferrara, Italy;
 (B) University of Ferrara, I-44122, Ferrara, Italy
 - ³⁰ Inner Mongolia University, Hohhot 010021, People's Republic of China
 - ³¹ Institute of Modern Physics, Lanzhou 730000, People's Republic of China
 - ³² Institute of Physics and Technology, Peace Avenue 54B, Ulaanbaatar 13330, Mongolia
 - ³³ Instituto de Alta Investigación. Universidad de Tarapacá. Casilla 7D. Arica 1000000. Chile
 - ³⁴ Jilin University, Changchun 130012, People's Republic of China
 - ³⁵ Johannes Gutenberg University of Mainz, Johann-Joachim-Becher-Weg 45, D-55099 Mainz, Germany
 - ³⁶ Joint Institute for Nuclear Research, 141980 Dubna, Moscow region, Russia
 - ³⁷ Justus-Liebig-Universitaet Giessen, II. Physikalisches Institut, Heinrich-Buff-Ring 16, D-35392 Giessen, Germany
 - ³⁸ Lanzhou University, Lanzhou 730000, People's Republic of China

- ³⁹ Liaoning Normal University, Dalian 116029, People's Republic of China
- ⁴⁰ Liaoning University, Shenyang 110036, People's Republic of China
- ⁴¹ Nanjing Normal University, Nanjing 210023, People's Republic of China
- ⁴² Nanjing University, Nanjing 210093, People's Republic of China
- ⁴³ Nankai University, Tianjin 300071, People's Republic of China
- ⁴⁴ National Centre for Nuclear Research, Warsaw 02-093, Poland
- ⁴⁵ North China Electric Power University, Beijing 102206, People's Republic of China
- ⁴⁶ Peking University, Beijing 100871, People's Republic of China
- ⁴⁷ Qufu Normal University, Qufu 273165, People's Republic of China
- ⁴⁸ Renmin University of China, Beijing 100872, People's Republic of China
- ⁴⁹ Shandong Normal University, Jinan 250014, People's Republic of China
- ⁵⁰ Shandong University, Jinan 250100, People's Republic of China
- ⁵¹ Shanghai Jiao Tong University, Shanghai 200240, People's Republic of China
- ⁵² Shanxi Normal University, Linfen 041004, People's Republic of China
- ⁵³ Shanxi University, Taiyuan 030006, People's Republic of China
- ⁵⁴ Sichuan University, Chengdu 610064, People's Republic of China
- ⁵⁵ Soochow University, Suzhou 215006, People's Republic of China
- ⁵⁶ South China Normal University, Guangzhou 510006, People's Republic of China
- ⁵⁷ Southeast University, Nanjing 211100, People's Republic of China
- ⁵⁸ State Key Laboratory of Particle Detection and Electronics, Beijing 100049, Hefei 230026, People's Republic of China
- ⁵⁹ Sun Yat-Sen University, Guangzhou 510275, People's Republic of China
- ⁶⁰ Suranaree University of Technology, University Avenue 111, Nakhon Ratchasima 30000, Thailand
- ⁶¹ Tsinghua University, Beijing 100084, People's Republic of China
- ⁶² Turkish Accelerator Center Particle Factory Group, (A) Istinye University, 34010, Istanbul, Turkey; (B) Near East University, Nicosia, North Cyprus, 99138, Mersin 10, Turkey
- ⁶³ University of Bristol, H H Wills Physics Laboratory, Tyndall Avenue, Bristol, BS8 1TL, U.K.
- ⁶⁴ University of Chinese Academy of Sciences, Beijing 100049, People's Republic of China
- ⁶⁵ University of Groningen, NL-9747 AA Groningen, The Netherlands
- ⁶⁶ University of Hawaii, Honolulu, Hawaii 96822, U.S.A.
- ⁶⁷ University of Jinan, Jinan 250022, People's Republic of China
- ⁶⁸ University of Manchester, Oxford Road, Manchester, M13 9PL, United Kingdom
- ⁶⁹ University of Muenster, Wilhelm-Klemm-Strasse 9, 48149 Muenster, Germany
- ⁷⁰ University of Oxford, Keble Road, Oxford OX13RH, United Kingdom
- ⁷¹ University of Science and Technology Liaoning, Anshan 114051, People's Republic of China
- ⁷² University of Science and Technology of China, Hefei 230026, People's Republic of China
- ⁷³ University of South China, Hengyang 421001, People's Republic of China
- ⁷⁴ University of the Punjab, Lahore-54590, Pakistan
- ⁷⁵ University of Turin and INFN, (A) University of Turin, I-10125, Turin, Italy;
 (B) University of Eastern Piedmont, I-15121, Alessandria, Italy; (C) INFN, I-10125, Turin, Italy
- ⁷⁶ Uppsala University, Box 516, SE-75120 Uppsala, Sweden
- ⁷⁷ Wuhan University, Wuhan 430072, People's Republic of China
- ⁷⁸ Yantai University, Yantai 264005, People's Republic of China
- ⁷⁹ Yunnan University, Kunming 650500, People's Republic of China
- ⁸⁰ Zheiiana University, Hanazhou 310027, People's Republic of China
- ⁸¹ Zhengzhou University, Zhengzhou 450001, People's Republic of China
- ^a Deceased
- ^b Also at the Moscow Institute of Physics and Technology, Moscow 141700, Russia
- c Also at the Novosibirsk State University, Novosibirsk, 630090, Russia
- ^d Also at the NRC "Kurchatov Institute", PNPI, 188300, Gatchina, Russia
- ^e Also at Goethe University Frankfurt, 60323 Frankfurt am Main, Germany
- f Also at Key Laboratory for Particle Physics, Astrophysics and Cosmology, Ministry of Education; Shanghai Key Laboratory for Particle Physics and Cosmology; Institute of Nuclear and Particle Physics, Shanghai 200240, People's Republic of China

- ^g Also at Key Laboratory of Nuclear Physics and Ion-beam Application (MOE) and Institute of Modern Physics, Fudan University, Shanghai 200443, People's Republic of China
- ^h Also at State Key Laboratory of Nuclear Physics and Technology, Peking University, Beijing 100871, People's Republic of China
- ⁱ Also at School of Physics and Electronics, Hunan University, Changsha 410082, China
- ^j Also at Guangdong Provincial Key Laboratory of Nuclear Science, Institute of Quantum Matter, South China Normal University, Guangzhou 510006, China
- ^k Also at MOE Frontiers Science Center for Rare Isotopes, Lanzhou University, Lanzhou 730000, People's Republic of China
- ¹ Also at Lanzhou Center for Theoretical Physics, Lanzhou University, Lanzhou 730000, People's Republic of China
- ^m Also at the Department of Mathematical Sciences, IBA, Karachi 75270, Pakistan
- ⁿ Also at Ecole Polytechnique Federale de Lausanne (EPFL), CH-1015 Lausanne, Switzerland
- ° Also at Helmholtz Institute Mainz, Staudinger Weg 18, D-55099 Mainz, Germany